Ann. Geophys., 29, 1731–1738, 2011
www.ann-geophys.net/29/1731/2011/
doi:10.5194/angeo-29-1731-2011

Annales Geophysicae

Three-dimensional spatial structures of solar wind turbulence from 10 000-km to 100-km scales

Y. Narita[1], K.-H. Glassmeier[1,2], M. L. Goldstein[3], U. Motschmann[4,5], and F. Sahraoui[6]

[1]Institut für Geophysik und extraterrestrische Physik, Technische Universität Braunschweig, Mendelssohnstr. 3, 38106 Braunschweig, Germany
[2]Max-Planck-Institut für Sonnensystemforschung, Max-Planck-Straße 2, 37191 Katlenburg-Lindau, Germany
[3]Geospace Physics Laboratory, Code 673, Goddard Space Flight Center, Greenbelt, MD 20771, USA
[4]Institut für Theoretische Physik, Technische Universität Braunschweig, Mendelssohnstr. 3, 38106 Braunschweig, Germany
[5]Deutsches Zentrum für Luft- und Raumfahrt, Institut für Planetenforschung, Rutherfordstr. 2, 12489 Berlin, Germany
[6]Laboratoire de Physique des Plasmas Observatoire de Saint-Maur, 4 avenue de Neptune, 94107 Saint-Maur-Des-Fossés, France

Received: 7 July 2011 – Accepted: 16 August 2011 – Published: 5 October 2011

Abstract. Using the four Cluster spacecraft, we have determined the three-dimensional wave-vector spectra of fluctuating magnetic fields in the solar wind. Three different solar wind intervals of Cluster data are investigated for this purpose, representing three different spatial scales: 10 000 km, 1000 km, and 100 km. The spectra are determined using the wave telescope technique (k-filtering technique) without assuming the validity of Taylor's frozen-in-flow hypothesis nor are any assumptions made as to the symmetry properties of the fluctuations. We find that the spectra are anisotropic on all the three scales and the power is extended primarily in the directions perpendicular to the mean magnetic field, as might be expected of two-dimensional turbulence, however, the analyzed fluctuations are not axisymmetric. The lack of axisymmetry invalidates some earlier techniques using single spacecraft observations that were used to estimate the percentage of magnetic energy residing in quasi-two-dimensional power. However, the dominance of two-dimensional turbulence is consistent with the relatively long mean free paths of cosmic rays in observed in the heliosphere. On the other hand, the spectra also exhibit secondary extended structures oblique from the mean magnetic field direction. We discuss possible origins of anisotropy and asymmetry of solar wind turbulence spectra.

Keywords. Interplanetary physics (Interplanetary magnetic fields; MHD waves and turbulence; Plasma waves and turbulence)

Correspondence to: Y. Narita
(y.narita@tu-bs.de)

1 Introduction

Investigating three-dimensional spatial structures is one of the most exciting tasks in studying the complex behavior of space plasma turbulence. There are several reasons for this: (1) various studies (observations and theories) suggest plasma turbulence to be anisotropic with respect to the ambient magnetic field; (2) determining spatial structure in three dimensions provides direct visualization that can give evidence of anisotropies; and (3) such a task is only possible with multi-spacecraft missions, such as Cluster (Escoubet et al., 2001). Solar wind turbulence serves as the only accessible, fully-developed plasma turbulence in space that allows detailed in-situ measurements using spacecraft. Studying the fluctuation properties of solar wind turbulence has immediate implications to astrophysical phenomena such as coronal heating, cosmic ray acceleration and propagation, as well as angular momentum transport in accretion disks.

The solar wind has various phases. The flow velocity observed at Earth's orbit (1 AU) varies typically between $300\,\mathrm{km\,s^{-1}}$ (slow wind) and $800\,\mathrm{km\,s^{-1}}$ (fast wind). The interplanetary magnetic field can point either away from the Sun or toward it, depending on the detailed structure of the corona from which the solar wind originates. Magnetic fluctuations in the solar wind are almost incompressible in the sense that the fluctuations are primarily perpendicular to the mean field and appear to be an example of fully-developed turbulence. Energy spectra of both magnetic field and flow velocity fluctuations often exhibit power law with indices close to $-5/3$ in the frequency domain (Coleman, 1968; Matthaeus and Goldstein, 1982; Matthaeus et al., 1982; Marsch and Tu, 1990; Podesta et al., 2007), which is

reminiscent of Kolmogorov's inertial-range spectrum of fluid turbulence. At frequencies around 0.1 Hz to 1 Hz, measurements further show a spectral break point where the spectrum steepens (Leamon et al., 1998; Smith et al., 2006) and is characterized by an index steeper than -2 (Behannon, 1978; Denskat et al., 1983; Goldstein et al., 1994; Leamon et al., 1998; Bale et al., 2005; Sahraoui et al., 2009). Recent analyses of Cluster data have shown that magnetic spectra in the range between 0.5 Hz and 2 Hz have an index between -2 to -4 (Sahraoui et al., 2009; Kiyani et al., 2009; Alexandrova et al., 2009), and suggest that there is another breakpoint above 20 Hz where the spectra become less steep before again steepening to about -4 as the fluctuations approach the electron inertial scale near 100 Hz (Sahraoui et al., 2009; Alexandrova et al., 2009).

Various studies suggest that plasma turbulence should be anisotropic. Earlier observations based on single spacecraft showed that correlation of magnetic field fluctuations in the solar wind tends to peak in directions both parallel and perpendicular to the mean magnetic field, and not in oblique directions (Matthaeus et al., 1990). Turbulent fluctuations in the solar wind are therefore often interpreted as a competition between two different fluctuation geometries. One is associated with wave vectors parallel to the mean magnetic field (referred to as the slab model because the fluctuations are primarily in a plane perpendicular to the background magnetic field), and the other is associated with perpendicular wave vectors (the two-dimensional turbulence model, in which the magnetic fields or flux tubes are distorted without being bent). Studies of cosmic ray transport also suggest that the two-dimensional turbulence geometry must play a dominant role to account for the long mean free paths of cosmic rays (Bieber et al., 1994, 1996). On the other hand, extensive correlation analyses using single spacecraft data suggest that the dominance of the two fluctuation geometries is case dependent: fluctuations described by the slab geometry dominate the fast streams and that of the two-dimensional turbulence geometry dominate the slow streams (Dasso et al., 2005).

The Cluster mission is unique in studying solar wind turbulence, since it can determine spatial structures (size and direction) of fluctuating fields in three dimensions without employing assumptions about symmetry or Taylor's frozen-in-flow hypothesis (Taylor, 1938). This paper is motivated by recent Cluster measurements of three-dimensional wave-vector spectra (Narita et al., 2010a; Sahraoui et al., 2010b) of fluctuating magnetic fields in the solar wind, which confirmed the existence of anisotropic energy spectra. These analyses concluded that there was a preference for two-dimensional turbulence. Furthermore, it was shown that axisymmetry in the spectrum is broken around the direction of the mean magnetic field. Here we use the analysis method developed by Sahraoui et al. (2006, 2010a) and Narita et al. (2010b) and investigate the three-dimensional structures of solar wind turbulence on three distinct scales: 10 000 km, 1000 km, and 100 km. These scales are important to understand the spatial structure of solar wind turbulence from the fluid to the ion kinetic regimes. On the spatial scale about 10 000 km the magnetohydrodynamic picture should be legitimate for describing solar wind turbulence, whereas on the scale about 100 km ion kinetics should play an important role as the ion gyro-radius and inertial length are of this order in the solar wind. In this paper, we cast the question if the energy spectra are anisotropic on these spatial scales.

2 Cluster measurements in the solar wind

2.1 Event selection

We chose three time intervals of solar wind data from Cluster fluxgate magnetometer experiment (FGM) (Balogh et al., 2001) for the analysis of the three-dimensional wave-vector spectra: (interval 1) 16 January 2006, 04:30–06:30 UT during the mission phase with about 10 000 km spacecraft separation; (interval 2) 21 March 2005, 18:00–20:00 UT with about 1000 km separation; (interval 3) 20 February 2002, 19:30–20:00 UT with about 100 km separation. These intervals were selected using the following criteria: (a) Cluster forms tetrahedron close to regular, which minimizes spectral distortion effects such as spatial aliasing and artificial anisotropies induced by irregular tetrahedron of sensor configuration (Narita et al., 2010b; Sahraoui et al., 2010a) in the analysis. For this purpose we set the minimum value for the tetrahedral configuration parameter, $Q_G \geq 2.5$. The parameter characterizes the tetrahedral shape such that one-dimensional array, two-dimensional plane, and three-dimensional regular tetrahedron formed by four points are given by the value 1.0, 2.0, and 3.0, respectively (von Stein et al., 1992; Robert et al., 1998). (b) The intervals contain very few discontinuities. (c) Fluctuations are weakly stationary, in the sense that the mean fields (magnetic field, flow velocity, and density) can be regarded as nearly constant (note that the strict stationarity requires more justification from power spectra and higher order moments of the probability density function. (d) The flow speed, the magnetic field magnitude, and the plasma beta are similar as shown in Table 1 to minimize the risk of mixing different solar wind phases, e.g. high-speed and low-speed streams. Figure 1 displays the time series plots of the magnetic field magnitude, solar wind speed, and ion density in the three intervals, respectively. Frequency spectra of magnetic field fluctuations (trace of the spectral density matrix in the spacecraft frame) exhibit the power-law with the index close to $-5/3$ at frequencies up to almost 1 Hz in all the three intervals (Fig. 2), confirming the typical power spectra in the solar wind in the low-frequency range.

Two points need to be addressed about the analyzed time intervals: electron foreshock activity and tetrahedral shape. The three intervals represent to large part the electron

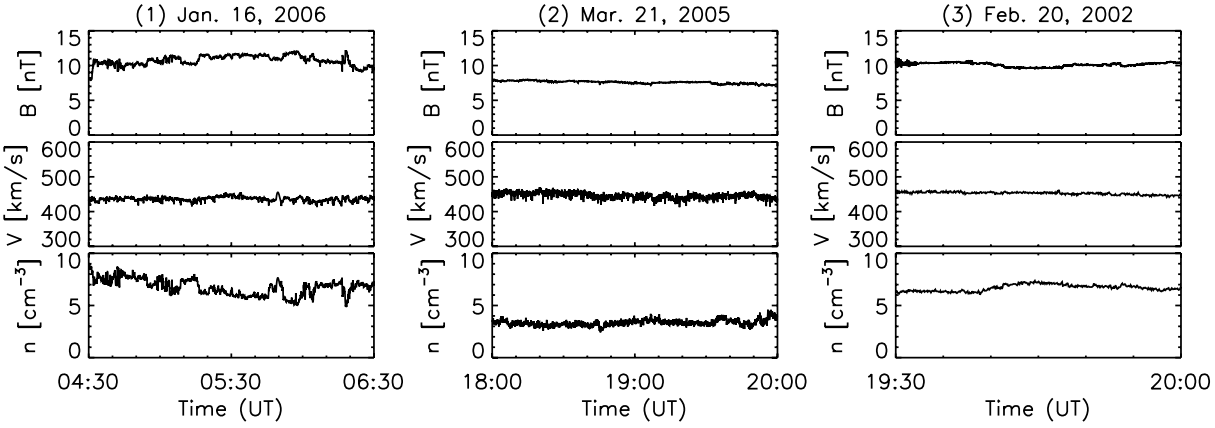

Fig. 1. Three time intervals displaying magnetic field magnitude, flow speed, and ion density in the solar wind. The data were obtained by fluxgate magnetometer (FGM) and electrostatic ion analyzer (CIS-HIA) on board Cluster-1 spacecraft.

Table 1. Mean values of plasma and magnetic field data in the three analyzed intervals: Characteristic tetrahedron size of Cluster L, flow speed V, ion number density n, magnitude of magnetic field $\boldsymbol{B}$, ion temperature T, and the plasma parameter beta.

Mean values	L	V	n	B	T	Beta
Units	km	km s^{-1}	cm^{-3}	nT	MK	1
Interval 1 (2006)	10 000	436.11	6.76	10.74	0.36	0.73
Interval 2 (2005)	1000	446.26	3.35	7.59	0.28	0.57
Interval 3 (2002)	100	443.05	6.69	10.13	0.32	0.72

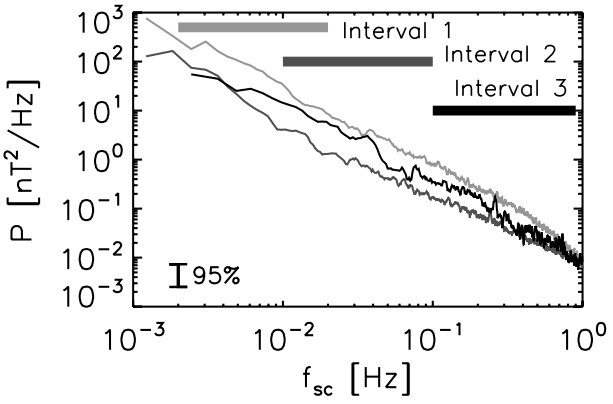

Fig. 2. Frequency spectra of magnetic field fluctuations in the three analyzed intervals: the upper curve in thin color is the spectrum for the interval 1, the lower curve the interval 2, and the middle curve in black the interval 3. The data are taken from fluxgate magnetometer on board Cluster, and the spectra are averaged over 4 spacecraft. Horizontal bars represent frequency ranges used in the wave vector analysis. Vertical bar with notation "95 %" at bottom left represents the confidence interval for the average number of sub-intervals used in the analysis.

foreshock as identified in high-frequency (2–80 kHz) electric field data from the WHISPER instrument (Décréau et al., 2001), although the intervals are uncontaminated by backstreaming ions associated with low-frequency foreshock activity. The interval 1 is the one that doesn't contain much electron foreshock activity, but the high-frequency wave data are nevertheless disturbed by the WHISPER sounding experiment. In addition, the spacecraft tetrahedral configuration is not strictly regular; planarity and elongation are not the smallest. Interpreting the fluctuation properties therefore needs special care. Quantitative analysis is performed to judge if the measured anisotropy is of natural origin and not "fake" anisotropies produced by irregular tetrahedron.

2.2 Data analysis

The three-dimensional wave-vector spectra were determined according to the procedure described in Narita et al. (2010b). In the first step, we determined the 12×12 cross spectral density (CSD) matrix in the frequency domain (in the spacecraft frame). Each element of the matrix represents cross-correlation of the magnetic field variation for different pairs of three components of the field measured at four spacecraft. For the interval 2 and 3, the data are split into 7 and 17 sub-intervals, respectively, and the CSD matrix is averaged over them for statistical significance. For the interval 1, one-hour sub-intervals are used for the analysis and averaged over sub-intervals slided by 1 min from the beginning to the end of the interval in order to resolve lower frequencies. Since Cluster performs measurements at spatially discrete points, the spatial aliasing effects must be taken into account in the wave-vector domain as well as in the frequency domain because the Doppler effect relating spatial and temporal variations brings about aliasing in the frequency domain, too. The CSD matrix was measured inside the principal distribution (i.e. the first Brillouin zone) in the wave vector domain determined by the spacecraft separation distance. The limit of frequency (in the

spacecraft frame) for the analysis is determined by investigating the periodic pattern of energy spectra in the frequency-wave vector domain (spatio-temporal aliasing). The limits of frequency in the spacecraft frame are 0.02 Hz, 0.1 Hz, and 1.0 Hz in intervals 1, 2, and 3, respectively.

In the second step, the CSD matrix is reduced into a 3×3 matrix (representing 3 components of the magnetic field) by projecting the matrix from the frequency domain into the four-dimensional frequency-wave vector domain using the wave telescope/k-filtering technique (Pinçon and Lefeuvre, 1991; Motschmann et al., 1996; Pinçon and Motschmann, 1998; Glassmeier et al., 2001). This technique is a generalization of array signal processing developed by Capon (1969), and represents a parametric approach of estimating power spectra in the wave-vector domain based on measurements only at several spatial points. In this projection method the filter coefficients are chosen so as to minimize the variance of the filter output under two constraints. The first is that the response of the filter is unity at the wave vector so as not to change the amplitude of waves by the projection, and the other is the divergence-free condition of the magnetic field. In the wave telescope technique, the wave vector serves as a parameter in the analysis, and the filter coefficients (projection weights) are determined not only by the wave vector but also by the measured CSD matrix itself for the purpose of reducing noise that comes from interference or cross-talk between different wave vectors in the spectral analysis.

The wave telescope technique can be regarded as a fitting procedure with propagating plane waves at various pairs of frequencies and wave vectors; this technique can determine the sign of wave vectors without use of cross helicity (which requires flow velocity data). Examples of distinguishing between forward and backward propagation directions using the wave telescope are displayed in Glassmeier et al. (2001) and Narita et al. (2009). In the spacecraft frame the accessible wave vectors are symmetric with respect to changing the sign. However, when the measurement is performed in a stream such as in the solar wind the accessible frequencies and wave vectors in the plasma rest frame (co-moving frame with the flow) become asymmetric between the flow direction and the opposite direction to it, which needs to be taken into account. The concept of the projection method for multi-point data analysis can further be applied to various fluctuation geometries, e.g. for spherical wave patterns (Constantinescu et al., 2006, 2007), and for phase-shifted wave patterns for field line resonances of geomagnetic fields (Plaschke et al., 2008).

In the third step, we obtain the fluctuation power by taking the trace of the reduced matrix as a function of frequencies and wave vectors in the spacecraft frame. The energy distribution is then transformed into the plasma rest frame by correcting for the Doppler shift. The mean flow velocity obtained by the electrostatic ion analyzer CIS-HIA on board Cluster (Rème et al., 2001) is used for the Doppler correction.

In the fourth step, the four-dimensional energy distribution is transformed into positive frequencies by changing the sign of frequencies and wave vectors for negative frequency components, and is then averaged over the rest-frame frequencies to obtain the three-dimensional wave-vector spectrum. The frequency averaging is performed in the range in which the spectrum is symmetrically covered (or measured) between the flow direction and its opposite direction in the plasma rest frame, in the range $\omega_{\rm rest} \leq 0.02\,{\rm rad\,s^{-1}}$ (interval 1), $\omega_{\rm rest} \leq 0.2\,{\rm rad\,s^{-1}}$ (interval 2), and $\omega_{\rm rest} \leq 1.0\,{\rm rad\,s^{-1}}$ (interval 3).

2.3 Results

Figure 3 displays the three-dimensional wave-vector spectra for the three intervals (and therefore on different spatial scales). For the purpose of comparison, the wave-vector ranges of the spectra are trimmed and presented as stereographic cubes with the maximum wave numbers $0.0001\,{\rm rad\,km^{-1}}$, $0.001\,{\rm rad\,km^{-1}}$, and $0.01\,{\rm rad\,km^{-1}}$ for the intervals 1, 2, and 3, respectively. The spectra are presented in the MFA (mean-field-aligned) coordinate system spanned by the mean magnetic field along the z-axis (the $k_\parallel$ axis) and the flow direction in the xz-plane (the $k_{\perp 1}$-$k_\parallel$-plane). The mean magnetic field and the flow velocity can be regarded as nearly constant within accuracy 1 % or even better. For representation, the three-dimensional distributions are averaged over the directions normal to the xy-, xz-, and yz-planes and displayed as three surfaces/contours on the cubes. Three-dimensional wave-vector spectra provide information on the symmetries and energy cascade directions (indicated by the extended structures of the spectra) in solar wind turbulence. We find the following symmetric or extension properties of the spectra.

On the spatial scale about 10 000 km (interval 1), the spectrum exhibits an anisotropic structure extended perpendicular to the mean magnetic field direction (left and right side panels, $k_{\perp 1}$-$k_\parallel$ and $k_{\perp 2}$-$k_\parallel$ planes). Furthermore, the spectrum is asymmetric around the mean field direction, too (top panel, $k_{\perp 1}$-$k_{\perp 2}$ plane). The spectrum is roughly symmetric with respect to changing the sign of the wave vector.

On the spatial scale about 1000 km (interval 2), the spectrum also exhibits an extended structure perpendicular to the mean field (left side panel, $k_{\perp 2}$-$k_\parallel$ plane). On the other hand, there is a moderate, secondary extended structure oblique from the mean field direction (right side panel, $k_{\perp 1}$-$k_\parallel$ plane). The axisymmetry around the mean field is broken and the spectrum is extended perpendicular to the flow direction (top panel, $k_{\perp 1}$-$k_{\perp 2}$ plane). The spectrum is again roughly symmetric with respect to changing the sign of the wave vector.

On the spatial scale about 100 km (interval 3), the spectrum exhibits more detailed structures: an elongated structure in the $k_{\perp 2}$ direction (left and top panels, $k_{\perp 2}$-$k_\parallel$ and $k_{\perp 1}$-$k_{\perp 2}$ planes); obliquely extended structures from the mean field (right panel, $k_{\perp 1}$-$k_\parallel$ plane). Around the direction of the mean

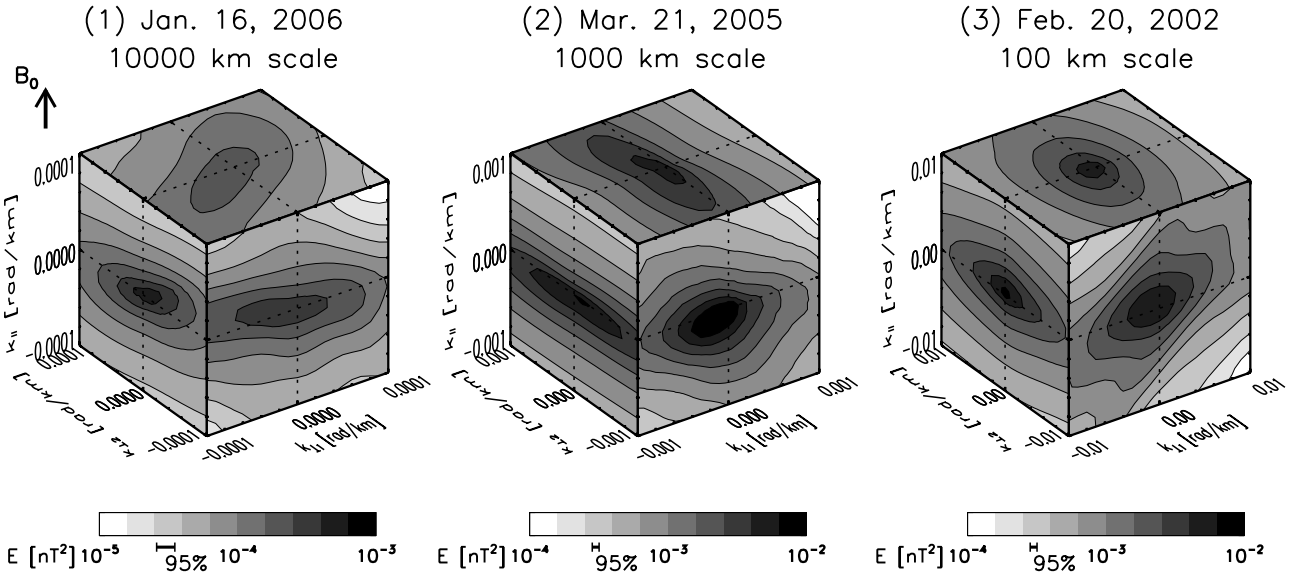

Fig. 3. Stereographic representation of the three-dimensional wave-vector spectra of fluctuating magnetic field in the solar wind for the three time intervals shown in Fig. 1. The spectra are presented in the MFA (mean-field-aligned) coordinate system spanned by the mean magnetic field (in the z-axis or $k_{\parallel}$-axis) and the flow direction (in the xz-plane or $k_{\perp 1}$-$k_{\parallel}$-plane) and averaged over the directions normal to the displayed plane. The confidence intervals at the color scales are based on the degree of freedom used for averaging over frequencies, wave numbers, and sub-intervals (for the interval 2 and 3).

magnetic field the spectrum is more gyrotropic than that in the interval 2, i.e. the asymmetry between the $k_{\perp 1}$ and $k_{\perp 2}$ components is weaker than that on the 1000 km scale. The spectrum is again nearly symmetric with respect to changing the sign of the wave vector. Interestingly, the oblique, extended structure in the $k_{\perp 1}$-$k_{\parallel}$ plane was found to be roughly perpendicular to the flow direction (about 100 degrees).

While the effects of irregular tetrahedron on the measurement of spectral anisotropy were minimized by event selection, the tetrahedral formation of the four spacecraft is not strictly regular in reality. It is therefore natural to ask if the detected anisotropies are physically relevant. Also, some of the recipcocal vectors happened to be nearly perpendicular to either the mean magnetic field direction or the flow direction. Angles of the longest reciprocal vectors of the tetrahedron are 106, 123, and 81 degrees from the mean magnetic field for interval 1, 2,3, respectively, and 59, 165, and 146 degrees from the flow direction. Angles of the shortest reciprocal vectors are 89, 50, and 41 degrees from the mean magnetic field, and 138, 97, and 118 degrees from the flow direction. For this purpose the measured anisotropies were evaluated quantitatively and compared with that caused by the irregular shape of tetrahedron using synthetic data. The anisotropy index A conveniently describes the elliptical shape of the spectrum in two dimensions, introduced by Shebalin et al. (1983) and later by Saito et al. (2008):

$$A = \frac{\Sigma_k k_a^2 E(k_a, k_b)}{\Sigma_k k_b^2 E(k_a, k_b)}, \quad (1)$$

where k_a and k_b denote the wave numbers in the maximum extended direction (or semi-major axis) and the minimum extended direction (semi-minor axis) in the two-dimensional spectrum, $E(k_a, k_b)$, respectively. Summation Σ_k is taken over k_a and k_b. This index essentially measures the ratio of the second order moments of the distribution (the width, namely) between the maximum and minimum extended directions by fitting the distribution with an ellipse. The values of the anisotropy index for the three planes ($k_{\perp 1}$-$k_{\perp 2}$, $k_{\perp 1}$-$k_{\parallel}$, and $k_{\perp 2}$-$k_{\parallel}$) are graphically presented in Fig. 4 as a function of the tetrahedron configuration parameter Q_G for the three time intervals.

The maximum anisotropy is found in the interval 2 (on 1000 km scale), $k_{\perp 2}$-$k_{\parallel}$-plane; and the minimum anisotropy in the interval 3 (on 10 000 km scale), $k_{\perp 1}$-$k_{\perp 2}$-plane. The values of the anisotropy index are separated from one plane to another in the three intervals. The average anisotropy index is about 2.0 in the $k_{\perp 1}$-$k_{\parallel}$ and $k_{\perp 2}$-$k_{\parallel}$ planes, and 1.6 in the $k_{\perp 1}$-$k_{\perp 2}$ plane. Error bars represent the variation of tetrahedral shape during the measurement (horizontal bars) and its effect on the anisotropy index (vertical bars, but they are smaller than the plotted symbol size). Dotted curve at the bottom in Fig. 4 represents anisotropy caused by the irregular shape of tetrahedron. Numerical test using synthetic data presented in Narita et al. (2010b) was extended to irregular, tetrahedral configuration at various values of Q_G. Synthetic data represent fluctuations with various frequencies and wave vectors characterized by isotropic energy distribution. The measurement itself causes anisotropy when

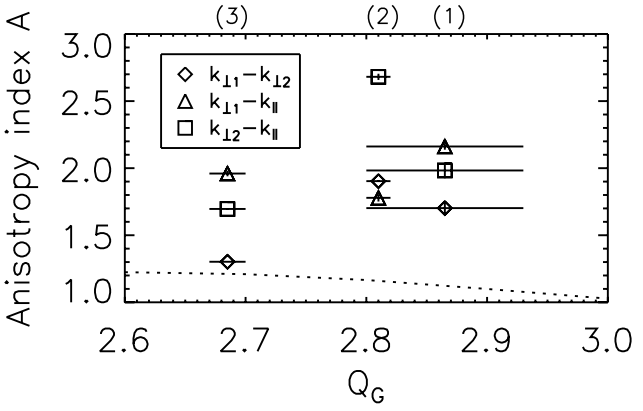

Fig. 4. Values of the anisotropy index as a function of the tetrahedral configuration parameter Q_G. The numbers (1)–(3) at the top of the panel denote the analyzed time interval. Three symbols denote the three projected planes in Fig. 3 for each time interval. Error bars reflect the variation of tetrahedral shape during the measurement. Dotted curve represent the artificial anisotropy produced by irregular tetrahedron.

the sensor tetrahedral configuration is not regular. This artificial anisotropy is larger at smaller values of Q_G (more irregular tetrahedron), and becomes minimum as the value of Q_G approaches to 3.0 (more regular tetrahedron). The artificial anisotropy is, however, at most about 1.2 for the tetrahedral configurations in the analyzed time intervals and is smaller than the measured values except for the $k_{\perp1}$-$k_{\perp2}$ plane in the interval 3. This justifies the anisotropy and asymmetry in field structure in solar wind turbulence most likely to be physically relevant.

3 Discussion and conclusions

To summarize the properties of the three-dimensional energy spectra, we find that anisotropy exists on all the three investigated scales from 10 000 km down to 100 km, and axially asymmetric, too. The anisotropy cannot be explained by the irregular tetrahedral shapes alone, and must reflect some physical mechanism in solar wind turbulence. It is interesting to compare our results with that derived from single spacecraft measurements. Podesta (2009) argues, for example, that the frequency spectrum of magnetic field fluctuations in the high-speed solar wind is approximately azimuthally symmetric about the mean field both in the inertial range (corresponding to 10 000 to 1000 km scales in our work) and dissipation/dispersion range (100 km in our work). The spatial structure of solar wind turbulence, in particular around the mean magnetic field, might be different between low-speed and high-speed streams. The three-dimensional energy spectra prefer extension primarily perpendicular to the mean magnetic field, and furthermore perpendicular to the mean flow direction on the intermediate and small scales (1000 and 100 km scales, respectively), too. The axisymmetry is broken around the mean magnetic field on these scales. The anisotropy between the parallel and the perpendicular directions becomes enhanced from the large scale (10 000 km) to the intermediate scale (1000 km), and then diminished on the small scale (100 km). The asymmetry in the plane perpendicular to the mean magnetic field becomes also enhanced from the large to the intermediate scale and diminished on the small scale. But it is not clear if the spectrum on the small scale (interval 3) is gyrotropic (axi-symmetric) or not, since the asymmetry might also be explained by the irregular tetrahedral shape.

It should be noted that the solar wind has different phases such as high- and low-speed streams, plasma parameter beta, and so on. The spectral anisotropy and asymmetry in our results should be extended to a variety of solar wind intervals of Cluster data including intervals with more regular tetrahedral configuration and also uncontaminated by electron foreshock activities.

The origin and mechanism of spectral anisotropy and asymmetry would be an interesting topic for understanding spatial and temporal structure of solar wind turbulence. Our data analysis shows that the spectral anisotropy prefers the sense of energy cascade perpendicular to the mean magnetic field, and there are several possible explanations: (1) the anisotropy already exists in the solar corona and it is simply transported by the solar wind, (2) it develops in the interplanetary space by scattering of Alfvén waves, or (3) it develops due to radial expansion of the solar wind in the heliosphere. Large-amplitude Alfvén waves are known to exist in the solar wind (Belcher and Davis, 1971) and theoretical studies have shown that large-amplitude Alfvén waves are subject to decay and modulational instabilities, collapsing into daughter waves (Goldstein, 1978; Longtin and Sonnerup, 1986; Terasawa et al., 1986; Wong and Goldstein, 1986). It is, however, questionable if these instabilities are relevant because they require a "pump" wave. Radial expansion of the solar wind may influence solar wind turbulence. Grappin (1996) demonstrated in numerical simulation that the expansion of the solar wind plasma causes stretching of eddies and anisotropy. As Roberts et al. (1987a,b) argued, large-scale inhomogeneity must be present in the solar wind and turbulence can actively be excited along with its divergent flow.

One may consider our results such that fluctuations in the N direction in the RTN coordinate system (pointing the direction of Sun's rotation axis in the solar equatorial plane) have no projection along the radial direction while fluctuations in the T direction do (perpendicular to the radial direction from the Sun and to Sun's rotatio axis). There may well be kinetic interaction with the δB_T component and not with δB_N. The simple implication would be not only non-axisymmetry but that the power in the N-direction would be greater than that in the T-direction. This expansion could, however, reduce power in the N direction more than in T, thus competing with the conjecture with the kinetic

interaction. Further studies of the three-dimensional spectra using Cluster data under various conditions of the solar wind and the tetrahedron sizes will verify our results and the possible causes of anisotropy.

Acknowledgements. This work was financially supported by Bundesministerium für Wirtschaft und Technologie and Deutsches Zentrum für Luft- und Raumfahrt, Germany, under contract 50 OC 0901.

Guest Editor A. Masson thanks S. P. Gary and J. Vogt for their help in evaluating this paper.

References

Alexandrova, O., Saur, J., Lacombe, C., Mangeney, A., Mitchell, J., Schawartz, S. J., and Rober, P.: Universality of solar wind turbulent spectrum from MHD to electron scale, Phys. Rev., Lett., 103, 165003, doi:10.1103/PhysRevLett.103.165003, 2009.

Bale, S. D., Kellogg, P. J., Mozer, F. S., Horbury, T. S., and Reme, H.: Measurement of the electric fluctuation spectrum of magnetohydrodynamic turbulence, Phys. Rev. Lett., 94, 215002, doi:10.1103/PhysRevLett.94.215002, 2005.

Balogh, A., Carr, C. M., Acuña, M. H., Dunlop, M. W., Beek, T. J., Brown, P., Fornacon, K.-H., Georgescu, E., Glassmeier, K.-H., Harris, J., Musmann, G., Oddy, T., and Schwingenschuh, K.: The Cluster Magnetic Field Investigation: overview of in-flight performance and initial results, Ann. Geophys., 19, 1207–1217, doi:10.5194/angeo-19-1207-2001, 2001.

Behannon, K. W.: Heliocentric distance dependence of the interplanetary magnetic field, Rev. Geophys., 16, 125–145, 1978.

Belcher, J. W. and Davis, L.: Large-amplitude Alfvén waves in the interplanetary medium, J. Geophys. Res., 76, 3534–3563, 1971.

Bieber, J. W., Matthaeus, W. H., Smith, C. W., Wanner, W., Kallenrode, M.-B., and Wibberenz, G.: Proton and electron mean free paths: The Palmer consensus revisited, Astrophys. J., 420, 294–306, 1994.

Bieber, J. W., Wannger, W., and Matthaeus, W. H.: Dominant two-dimensional solar wind turbulence with implications for cosmic ray transport, J. Geophys. Res., 101, 2511–2522, 1996.

Capon, J.: High resolution frequency-wavenumber spectrum analysis, Proc. IEEE, 57, 1408–1418, 1969.

Coleman Jr., P. J.: Turbulence, viscosity, and dissipation in the solar-wind plasma, Astrophys. J., 153, 371–388, 1968.

Constantinescu, O. D., Glassmeier, K.-H., Motschmann, U., Treumann, R. A., Fornaçon, K.-H., and Fränz, M.: Plasma wave source location using CLUSTER as a spherical wave telescope, J. Geophys. Res., 111, A09221, doi:10.1029/2005JA011550, 2006.

Constantinescu, O. D., Glassmeier, K.-H., Décréau, P. M. E., Fränz, M., and Fornaçon, K.-H.: Low frequency wave sources in the outer magnetosphere, magnetosheath, and near Earth solar wind, Ann. Geophys., 25, 2217–2228, doi:10.5194/angeo-25-2217-2007, 2007.

Dasso, S., Milano, L. J, Matthaeus, W. H., and Smith, C. W.: Anisotropy in fast and slow solar wind fluctuations, Astrophys. J., 635, L181–L184, 2005.

Décréau, P. M. E., Fergeau, P., Krasnoselskikh, V., Le Guirriec, E., Lévêque, M., Martin, Ph., Randriamboarison, O., Rauch, J. L., Sené, F. X., Séran, H. C., Trotignon, J. G., Canu, P., Cornilleau, N., de Féraudy, H., Alleyne, H., Yearby, K., Mögensen, P. B., Gustafsson, G., André, M., Gurnett, D. C., Darrouzet, F., Lemaire, J., Harvey, C. C., Travnicek, P., and Whisper experimenters: Early results from the Whisper instrument on Cluster: an overview, Ann. Geophys., 19, 1241–1258, doi:10.5194/angeo-19-1241-2001, 2001.

Denskat, K. U., Beinroth, H. J., and Neubauer, M. F.: J. Geophys, 54, 60–67, 1983.

Escoubet, C. P., Fehringer, M., and Goldstein, M.: Introduction: The Cluster mission, Ann. Geophys., 19, 1197–1200, doi:10.5194/angeo-19-1197-2001, 2001.

Glassmeier, K.-H., Motschmann, U., Dunlop, M., Balogh, A., Acuña, M. H., Carr, C., Musmann, G., Fornaçon, K.-H., Schweda, K., Vogt, J., Georgescu, E., and Buchert, S.: Cluster as a wave telescope – first results from the fluxgate magnetometer, Ann. Geophys., 19, 1439–1447, doi:10.5194/angeo-19-1439-2001, 2001 (correction in 21, 1071, 2003).

Goldstein, M. L.: An instability of finite amplitude circularly polarized Alfvén waves, Astrophys. J., 219, 700–704, 1978.

Goldstein, M. L., Roberts, D. A., and Fitch, A. C.: Properties of the fluctuating magnetic helicity in the inertial and dissipation ranges of solar wind turbulence, J. Geophys. Res., 99, 11519–11538, 1994.

Grappin, R.: Onset of anisotropy and Alfvén waves turbulence in the expanding solar wind, Solar Wind Eight, edited by: Winterhalter, D., Gosling, J. T., Habbal, S. R., Kurth, W. S., and Neugebauer, M., AIP Conference Proceedings, 382, pp. 306–309, 1996.

Kiyani, K. H., Chapman, S. C., Khotyaintsev, Y. V., Dunlop, M. W., and Sahraoui, F.: Global scale-invariant dissipation in collisionless plasma turbulence, Phys. Rev. Lett., 103, 075006, doi:10.1103/PhysRevLett.103.075006, 2009.

Leamon, R. J., Smith, C. W., Ness, N. F., Matthaeus, W. H., and Wong, H. K.: Observational constraints on the dynamics of the interplanetary magnetic field dissipation range, J. Geophys. Res., 103, 4775–4787, 1998.

Longtin, M. and Sonnerup, B.: Modulational instability of circularly polarized Alfvén waves, J. Geophys. Res., 91, 798–801, 1986.

Marsch, E. and Tu, C.-Y.: On the radial evolution of MHD turbulence in the inner heliosphere, J. Geophys. Res., 95, 8211–8229, 1990.

Matthaeus, W. H. and Goldstein, M. L.: Measurement of the rugged invariants of magnetohydrodynamic turbulence in the solar wind J. Geophys. Res., 87, 6011–6028, 1982.

Matthaeus, W. H., Goldstein, M. L., and Smith, C.: Evaluation of magnetic helicity in homogeneous turbulence, Phys. Rev. Lett., 48, 1256–1259, 1982.

Matthaeus, W. H., Goldstein, M. L., and Roberts, D. A.: Evidence for the presence of quasi-two-dimensional nearly incompressible fluctuations in the solar wind, J. Geophys. Res., 95, 20673–20683, 1990

Motschmann, U., Woodward, T. I., Glassmeier, K. H., Southwood, D. J., and Pinçon, J. L.: Wavelength and direction filtering by magnetic measurements at satellite arrays: Generalized minimum variance analysis, J. Geophys. Res., 101, 4961–4966, 1996.

Narita, Y., Kleindienst, G., and Glassmeier, K.-H.: Evaluation of magnetic helicity density in the wave number domain using multi-point measurements in space, Ann. Geophys., 27, 3967–3976, doi:10.5194/angeo-27-3967-2009, 2009.

Narita, Y., Glassmeier, K.-H., Sahraoui, F., and Goldstein,

M. L.: Wave-vector dependence of magnetic-turbulence spectra in the solar wind, Phys. Rev. Lett., 104, 171101, doi:10.1103/PhysRevLett.104.171101, 2010a.

Narita, Y., Sahraoui, F., Goldstein, M. L., and Glassmeier, K.-H.: Magnetic energy distribution in the four-dimensional frequency and wave vector domain in the solar wind, J. Geophys. Res., 115, A04101, doi:10.1029/2009JA014742, 2010b.

Pinçon, J. L. and Lefeuvre, F.: Local characterization of homogeneous turbulence in a space plasma from simultaneous measurements of field components at several points in space, J. Geophys. Res., 96, 1789–1802, 1991.

Pinçon, J.-L. and Motschmann, U.: Multi-Spacecraft Filtering: General Framework, Analysis Methods for Multi-Spacecraft Data, edited by: Paschmann, G. and Daly, P. W., ISSI Sci. Rep. SR-001, chap. 3, pp. 65–78, International Space Science Institute, Berne, Switzerland, 1998.

Plaschke, F., Glassmeier, K.-H., Constantinescu, O. D., Mann, I. R., Milling, D. K., Motschmann, U., and Rae, I. J.: Statistical analysis of ground based magnetic field measurements with the field line resonance detector, Ann. Geophys., 26, 3477–3489, doi:10.5194/angeo-26-3477-2008, 2008.

Podesta, J. J.: Dependence of solar-wind power spectra on the direction of the local mean magnetic field, Astrophys. J., 698, 986–999, doi:1.1088/0004-637X/698/2/986, 2009.

Podesta, J. J., Roberts, D. A., and Goldstein, M. L.: Spectral exponents of kinetic and magnetic energy spectra in solar wind turbulence, Astrophys. J., 664, 543–548, doi:10.1086/519211, 2007.

Rème, H., Aoustin, C., Bosqued, J. M., Dandouras, I., Lavraud, B., Sauvaud, J. A., Barthe, A., Bouyssou, J., Camus, Th., Coeur-Joly, O., Cros, A., Cuvilo, J., Ducay, F., Garbarowitz, Y., Medale, J. L., Penou, E., Perrier, H., Romefort, D., Rouzaud, J., Vallat, C., Alcaydé, D., Jacquey, C., Mazelle, C., d'Uston, C., Möbius, E., Kistler, L. M., Crocker, K., Granoff, M., Mouikis, C., Popecki, M., Vosbury, M., Klecker, B., Hovestadt, D., Kucharek, H., Kuenneth, E., Paschmann, G., Scholer, M., Sckopke, N., Seidenschwang, E., Carlson, C. W., Curtis, D. W., Ingraham, C., Lin, R. P., McFadden, J. P., Parks, G. K., Phan, T., Formisano, V., Amata, E., Bavassano-Cattaneo, M. B., Baldetti, P., Bruno, R., Chionchio, G., Di Lellis, A., Marcucci, M. F., Pallocchia, G., Korth, A., Daly, P. W., Graeve, B., Rosenbauer, H., Vasyliunas, V., McCarthy, M., Wilber, M., Eliasson, L., Lundin, R., Olsen, S., Shelley, E. G., Fuselier, S., Ghielmetti, A. G., Lennartsson, W., Escoubet, C. P., Balsiger, H., Friedel, R., Cao, J.-B., Kovrazhkin, R. A., Papamastorakis, I., Pellat, R., Scudder, J., and Sonnerup, B.: First multispacecraft ion measurements in and near the Earth's magnetosphere with the identical Cluster ion spectrometry (CIS) experiment, Ann. Geophys., 19, 1303–1354, doi:10.5194/angeo-19-1303-2001, 2001.

Robert, P., Roux, A., Harvey, C. C., Dunlop, M. W., Daly, P. W., and Glassmeier, K.-H.: Tetrahedron geometric factors, in: Analysis Methods for Multi-Spacecraft Data, pp. 323–348, ISSI Scientific Report SR-001, edited by: Paschmann, G. and Daly, P. W., International Space Science Institute, ISSI/ESA, 1998.

Roberts, D. A., Goldstein, M. L., Klein, L. W., and Matthaeus, W. H.: Origin and evolution of fluctuations in the solar wind: Helios observations and Helios-Voyager comparison, J. Geophys. Res., 92, 12023–12035, 1987a.

Roberts, D. A., Klein, L. W., Goldstein, M. L., and Matthaeus, W. H.: The nature and evolution of magnetohydrodynamic fluctuation in the solar wind: Voyager observations J. Geophys. Res., 92, 11021–11040, 1987b.

Sahraoui, F., Belmont, G., Rezeau, L., Cornilleau-Wehrlin, N., Pinçon, J. L., and Balogh, A.: Anisotropic turbulent spectra in the terrestrial magnetosheath as seen by the Cluster spacecraft, Phys. Rev. Lett., 96, 075002, doi:10.1103/PhysRevLett.96.075002, 2006.

Sahraoui, F., Goldstein, M. L., Robert, P., and Khotyaintsev, Yu. V.: Evidence of a cascade and dissipation of solar-wind turbulence at the electron gyroscale, Phys. Rev. Lett., 102, 231102, doi:10.1103/PhysRevLett.102.231102, 2009.

Sahraoui, F., Belmont, G., Goldstein, M. L., and Rezeau, L.: Limitations of multispacecraft data techniques in measuring wave number spectra of space plasma turbulence, J. Geophys. Res., 115, A04206, doi:10.1029/2009JA014724, 2010a.

Sahraoui, F., Goldstein, M. L., Belmont, G., Canu, P., and Rezeau, L.: Three dimensional anisotropic k spectra of turbulence at subproton scales in the solar wind, Phys. Rev. Lett., 105, 131101, doi:10.1103/PhysRevLett.105.131101, 2010b.

Saito, S., Gary, S. P., Li, H., and Narita, Y.: Whistler turbulence: Particle-in-cell simulations, Phys. Plasmas, 15, 102305, doi:10.1063/1.2997339, 2008.

Shebalin, J. V., Matthaeus, W. H., and Montgomery, D.: Anisotropy in MHD turbulence due to a mean magnetic field, J. Plasma Phys, 29, 525–547, 1983.

Smith, C. W., Hamilton, K., Vasquez, B. J., and Leamon, R. J.: Dependence of the dissipation range spectrum of interplanetary magnetic fluctuations on the rate of energy cascade, Astrophys. J., 645, L85, doi:10.1029/2006JA011651, 2006.

Taylor, G. I.: The spectrum of turbulence, Proc. R. Soc. Lond. A, 164, 476–490, 1938.

Terasawa, T., Hoshino, M., Sakai, J.-I., and Hada, T.: Decay instability of finite-amplitude circularly polarized Alfvén waves: A numerical simulation of stimulated brillouin scattering, J. Geophys. Res., 91, 4171–4187, 1986.

von Stein, R., Glassmeier, K.-H., and Dunlop, M.: A configuration parameter for the Cluster satellites, Tech. Rep. 2/1992, Institut für Geophysik und Meteorologie der Technischen Universität Braunschweig, 1992.

Wong, H. K. and Goldstein, M. L.: Parametric instabilities of circularly polarized Alfvén waves including dispersion, J. Geophys. Res., 91, 5617–5628, 1986.